Optical poling of oligoether acrylate photopolymers doped by stilbene-benzoate derivative chromophores

I V Kityk[1]**, M Makowska-Janusik**[1]**, E Gondek**[2]**, L Krzeminska**[3]**,
A Danel**[3]**, K J Plucinski**[4]**, S Benet**[5] **and B Sahraoui**[6]

[1] Institute of Computer Modeling, Krakow Technological University, ulica Warszawska 24, Krakow, Poland
[2] Institute of Physics, Cracow University of Technology, ulica Podchorazych 1, 30-084 Krakow, Poland
[3] Departament of Chemistry, Agricultural University, aleja Mickiewicza 24/28, 30-059 Krakow, Poland
[4] Military University of Technology, ulica Kaliskiego 4, Warsaw, Poland
[5] Laboratoire LP2A, boulevard Villeuve 58, Universite de Perpignan, France
[6] Laboratoire POMA, Universite d'Angers, Angers, France

E-mail: i.kityk@wsp.czest.pl

Abstract
A large second harmonic generation (SHG) excited by an Nd:YAG laser ($\lambda = 1.32\ \mu$m) has been observed during the investigation of the optical poling process in 2-(stilbene-4-yl)benzoxazole derivatives chromophores incorporated within oligoether acrylate photopolymer matrices. We have revealed that the maximum output SHG is observed for the chromophore derivatives molecule possessing the highest second-order hyperpolarizabilities and corresponding dipole moments. Due to the incorporation of the chromophore into photopolymer matrices, second-order microscopic susceptibilities of the composites substantially increase (from 0.24 up to 1.89 pm V^{-1}). The investigated composites possess long-lived polarized states and after more than 10^6 laser pulses the output SHG did not decrease below 75% compared with the initial SHG one. Optimal conditions for optical poling corresponded to a power density of the doubled frequency beam of about 0.07 GW cm^{-2} and chromophore content about 6.5% (in weighting units).

(Some figures in this article are in colour only in the electronic version)

1. Introduction

During long illumination of a randomly oriented disordered medium (glass, amorphous-like materials, polymers, etc) by two coherent sources possessing different frequencies (ω and 2ω) one can observe the appearance of reversible long-lived static polarization inside the medium [1–7]. The value of the polarization will be determined [8, 9] by the formation of

a spatially periodic electrostatic field $\mathbf{E}(\mathbf{r})$ in the medium under the action of the bicolour coherent light and by the second-order optical susceptibilities. This effect is usually called the all optical poling or $\chi^{(2)}$ optical grating. Due to the loss of its symmetry (or random-oriented centrosymmetry) there appear properties of a uniaxial crystal with photoinduced optical axes determined by the light polarization of the pumping beam. At the same time there occurs an optical ellipsoid of refractive indices corresponding to uniaxial crystal symmetry. A general physical conception of the interactions was described in [10, 11]. As a result, the optically-induced second harmonic generation (SHG) and parametric amplification or parametrization of light become possible in such an optically perturbed medium. The main goal of the present work is to investigate the possibility of a substantial increase of the output optically-poled SHG during such kinds of experiment. Hence photoinduced SHG, first observed by Österberg and Margulis [1], has been investigated intensively for more than 15 years in germanium-silicate fibres and different bulk oxide glasses; unfortunately, the maximal efficiency of the SHG (about 5%), which was obtained in the first work [1] in a germanium-silicate fibre, is the maximum obtained to date. The main factor which substantially restrains a wider application of the optical poling consists of the fact that silicon or germanium [12] glasses which usually are used for the optical poling do not possess enough second-order susceptibility coefficients, which makes the output SHG poorly efficient ($<10^{-2}$) compared with the best non-linear crystals such as β-BBO, BiBO or KTP. At the same time the azo-dye red chromophores [13] are not sufficiently stable against the temperature and photochemical treatment.

In contrast to the crystals, optical poling has a substantial advantageous requirement that the phase-matching conditions for the SHG can be automatically satisfied.

In our opinion one promising way to enhance the local non-linear optical susceptibility consists of fabrication of host–guest photopolymer matrices possessing the electrically-aligned embedded chromophores. In [14] we have shown that even non-coherent photoinduced SHG in different organic materials is substantially higher than in inorganic ones. Additional electric alignment during the photopolymerized solidification may additionally favour the observed effect.

We expect that the host–guest technique including the chromophore molecule incorporated within the photopolymer matrices [14] may present a particular interest because it connects the advantages of the organic molecular π-conjugate chromophore–matrix transfer and the time stability of the composites due to the electrically-aligned solidified process, compared with the azo-dye chromophores.

In the present paper the results of the observation of the photoinduced SHG phenomenon which appears during the optical poling of 2-(stilben-4-yl)benzoxazole derivatives (see figure 1) incorporated in oligoetheracrylate (OEA) photopolymer matrices [15] are presented. During the investigation of the optical poling process, a large increase of the output optical SHG is observed. These chromophores are used as materials for visible light emitting diodes [16].

Because these compounds have large emission and electroluminescent bands below 600 nm, as a source of fundamental laser beams we have chosen the 1.32 μm Nd:YAG laser wavelength with pulse duration of about 25 ps. Using β-BBO single crystals we have obtained simultaneously optical SHG for a wavelength of about 0.66 μm. The absorption spectra of these compounds which we will indicate by **1**–**3** are presented in figure 2. The number **1** will correspond in the figure 1 to X=H; **2**—to phenyl and **3**—to O–Me groups.

One can conclude that both the absorption and the luminescent bands are spectrally separated with respect to the fundamental and doubled-frequency wavelengths.

In section 2 we will present experimental details of the chemical synthesis of the compounds and measurement set-up. In section 3 the main results will be given and an appropriate discussion will be presented.

1

2

3
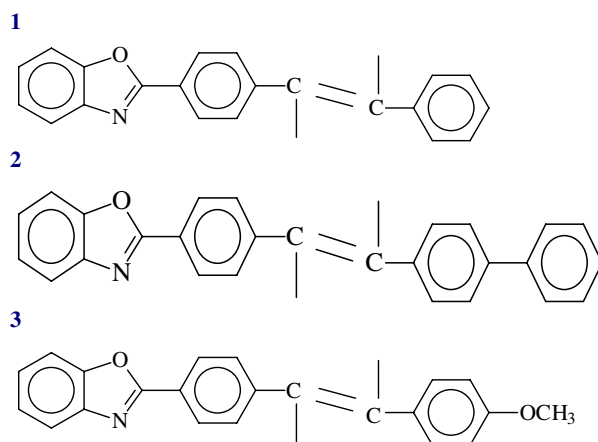
Figure 1. The general chemical formula of the stilbene-benzoate derivative chromophore molecule: **1**—H; **2**—phenyl; **3**—OMe.
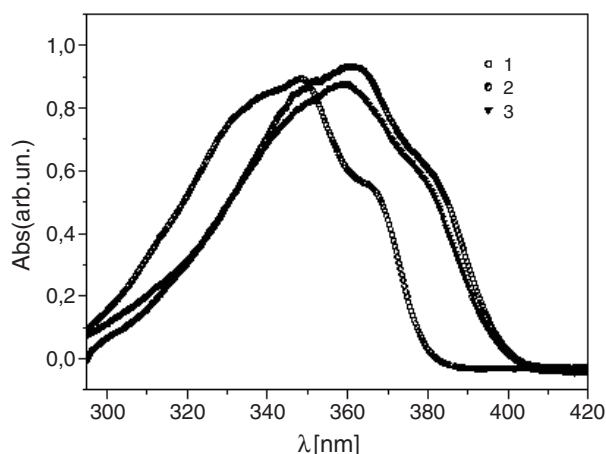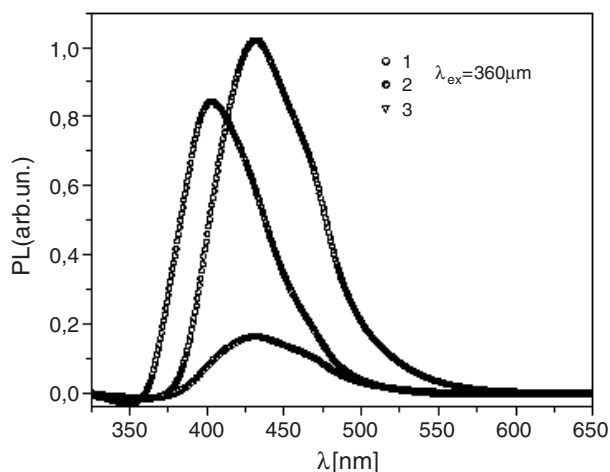

Figure 2. Absorption spectra of the investigated chromophores.

2. Experimental details

The 2-(stilben-4-yl)benzoxazole derivatives **1**–**3** to be investigated were prepared following the Anilm synthesis reported by Siergrist [17]. 2-(p-tolyl)-benzoxazole (0.01 mol) and the Shiff base of the appropriate aromatic benzaldehyde were dissolved in anhydrous DMF and potassium tert-butoxide (0.015 mol). The reaction mixture was stirred at 50 °C for 3 h. After cooling it was poured into water and acidified with 10% HCl. The precipitate was filtered off, dried, and recrystallized from DMF. The products were characterized by NMR and compared with reference data.

Chromophore **1**—*(stilbene-4-yl)-benzoxazole*. Colourless powder, mp 198.6 °C; ^{1}H NMR (300 MHz, CDCl3): δ 7.14 (d, $J = 16.2$ Hz, 1H), d, $J = 16.5$ Hz, 1H), 7.23 (d, $J = 16.5$ Hz, 1H), 7.30 (t, $J = 7.4$ Hz, 1H), 7.34–7.41 (m, 4H), 7.55 (d, $J = 8.2$ Hz, 2H), 7.76–7.79 (m, 1H), 8.23 (d, $J = 8.5$ Hz, 2H). Chromophore **2**—4-*(phenylstilben-4′-yl)-benzoxazole*. Green powder, mp 275 °C; ^{1}H NMR (300 MHz, DMSO): δ 7.34–7.43 (m, 7H), 7.68–7.80 (m, 8H), 7.83 (d, $J = 8.2$ Hz, 2H), 8.19 (d, $J = 8.2$ Hz, 2H).

Figure 3. Emission spectra of the investigated chromophores.

Chromophore **3**—4-*(methoxystilben-4′-yl)-benzoxazole*. Yellow needles, mp 218.5 °C; ^{1}H NMR (300 MHz, CDCl$_3$): δ 3.84 (s, 3H, OCH$_3$), 6.92 (d, $J = 8.5$ Hz, 2H), 7.02 (d, $J = 16.2$ Hz, 1H), 7.02 (d, $J = 16.2$ Hz, 1H), 7.33–7.36 (m, 2H), 7,49 (d, $J = 8.8$ Hz, 2H), 7.55–7.60 (m, 1H), 7.63 (d, $J = 8.5$ Hz, 2H), 7.74–7.80 (m, 1H), 8.23 (d, $J = 8.5$ Hz, 2H).

The OEA liquid photocomposition was prepared in accordance with [15, 18]. From figures 2 and 3 one can see that the absorption and luminescent spectra lie below 600 nm. A shift in the spectral position of the luminescence is used in the production of light emitting diodes. So we can have composites simultaneously possessing good visible emitting properties as well as properties typical for non-linear optical materials.

The synthesized molecules with the formulae shown in figure 1 were in the form of powder and were dissolved in the liquid OEA photocomposition in the appropriate weight proportion. Afterwards the composite was mixed in an external acoustical field in order to obtain a homogenous space distribution of the chromophore. Solidification was performed using a low-power continuous nitrogen laser with wavelength 337 nm possessing power density about 45 W cm^{-2}. Transparent ITO electrodes were applied for the creation of long-range ordering due to alignment of the powder. More details concerning the UV-solidification are given in [19].

The optically-induced experiment was similar to that described in [12]. The axially-symmetry beam sequence of the fundamental YAlO$_3$:Nd^{3+} laser ($\lambda = 1.32\,\mu$m) and its doubled harmonic obtained by the BBO crystal cut in the phase matching angle were focused inside the sample in the central part of the concentric circle. The duration of pulses was 500 ps, the pulse energy was 2.1 mJ, and the repetition frequency was about 10 Hz. The fundamental wavelength was converted into the doubled frequency ($\lambda \approx 0.66\,\mu$m) by the BBO crystal with conversion efficiency 22%. The diameter of the beams at the focal point was $\sim$60–68 μm, and the intensity at the waist was $I_\omega \sim 5.2$ GW cm^{-2} and $I_{2\omega} \sim 1.1$ GW cm^{-2} for the fundamental and doubled harmonics, respectively. The set of mirrors and lenses allow operation of the beam parameters, and the shutters switch off several beams at the desired moment of time. Using the lenses we vary the diameters of the beams and the green filters are served for the spectral separation of the green second harmonic signals from the fundamental beam. The photomultiplier PM works in the fast-response regime (about 0.6 ns) and is connected to the electronic boxcar integrator **EB**. The incident angles of the two beams on the sample make a small angle (about 4°–5°)
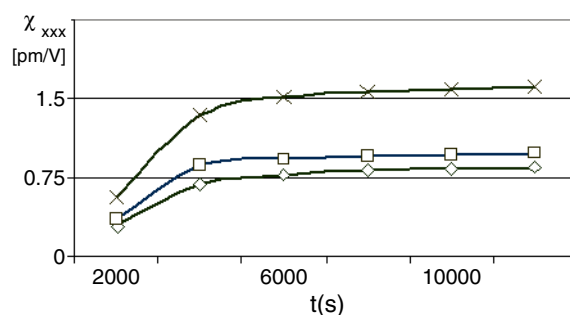
Figure 4. The dependence of the output SHG on the time of illumination by 2ω writing beam: ×—chromophore **3**; □—chromophore **2**; ◇—chromophore **1**. The concentration of the chromophore molecule is equal to about 6.5% (in weight units). The writing beam power density is equal to about 0.074 GW cm^{-2}.

with respect to the sample's surface normal. This one allows to vary the grating period within the 18–28 μm. The polarizations of the beams were linear and were directed perpendicular to the **k**-wavevector of the beam propagation.

During this illumination of composites with coherent two-frequency radiation (during the optical poling of composites [5]) the electrostatic field grating **E**(**r**) and, correspondingly, $\chi^{(2)}$-grating were created in the space region of the beam's overlap. The efficient coherence length of the composites was varied within 18–28 μm depending on the type and concentration of chromophore.

The conversion of the fundamental frequency beam into PISHG output radiation takes place on the accumulative $\chi^{(2)}$-grating. The propagation of the photoinduced SHG is in the direction of propagation of the incident beam with the doubled frequency (the so-called writing beam). For the registration of the photoinduced SHG we eliminate the incident (writing) signal at the entrance to the sample for short time intervals of 0.2 s every 1–1.5 min. Finally we measure the peak power $I_{SHG}(2\omega)$ of the photoinduced SHG on the $\chi^{(2)}$-grating using an RCA photomultiplier in the remote zone. Afterwards the signals were integrated by the electronic boxcar integrator **EB**. The output SHG signals were statistically averaged over 12–16 SHG pulses to reduce the influence of the SHG signal instability. In addition we have used a separate fast-time photodiode for the monitoring of laser stability. The power density sensitivity threshold of the set-up was about 0.3 μW/pulse. The set-up allows us to perform monitoring of the fundamental and output SHG signal simultaneously.

3. Results and discussions

In figure 4 the time dependence of the efficiency of SHG χ_{xxx} versus the time of treatment by the incident beam with the doubled frequency 2ω is shown. For convenience the results are presented for optimal writing doubled-frequency peak powers (about 0.075 GW cm^{-2}). One can see that the maximal output is observed for the molecule **3**, containing the OHMe group. The maximum SHG output signal corresponded to the chromophore content of about 6.5% (in weight units). The evaluations of the effective second-order susceptibility at these wavelengths show that within the photopolymer hosts the output second-order susceptibility seems to be about 1.6 pm V^{-1}, which corresponds to the chromophore–polymer π-conjugations, giving substantial contribution to the output susceptibility. It is important to emphasize that there exists a correlation between the values of chromophore state dipole moments and of the

Table 1. Calculated dipole moments for different chromophore molecules calculated by the method described in [20].

Type of chromophore	Dipole moment (D) For isolated molecule	Dipole moment (D) For molecule incorporated within the OEA matrices
1	1.27	9.8
2	1.56	11.7
3	2.6	24.8

output second-order susceptibilities. In particular, our calculations performed using the semi-empirical quantum chemical AM1 method show that the state dipole moments (see table 1) on the border chromophore–polymer increase by at least one order, which may lead to a substantial increase of the susceptibility. The evaluations were done taking into account the inter-border MM + force field molecular dynamics method together with the quasi-solid-state approach introduced in [20]. The samples investigated were of parallelepiped shape, from $0.5 \times 0.5 \times (0.1–0.3)$ mm. So taking into account the actual coherence length of the composites (about 20–28 μm), we are able to observe an output PISHG within the Maker fringence experiment at quasi-phase matched conditions.

The further increase of the second-order susceptibility with increasing chromophore content is limited by the occurrence of chromophore agglomerates, which substantially limit the output of effective susceptibilities. This limitation may be caused by carrier diffusion [12].

This correlates well with the microscopic local hyperpolarizability calculated using the semi-empirical AM1 method and oversimplified two-level model. Comparing the values of the state dipole moments with the output SHG, one can observe a striking correlation. In particular, in our case a great contribution may be given by the guest–host borders, which are crucially efficient in the case of the quasi-collinear dipole moments for the chromophore and surrounding photopolymer. The latter one in our case is achieved additionally by the appropriate application of an aligned electric field to the particular molecule.

The optical poling has substantial advantages compared with electric-field or corona poling, consisting of the possibility of satisfying the phase-matching conditions without the necessity of using electrodes. In contrast to the azo-dye chromophores, the investigated composites do not break long-range ordering due to orientation relaxation. So we try using the guest–host technique both to improve the stability of the $\chi^{(2)}$-grating forming process as well as to enhance its efficiency, which should be manifested through the decrease of time during which the optical poling process achieves its saturation, determined by the corresponding steady-state processes.

The maximal increase of the output PISHG is observed during the first 5000 s of laser treatment. The obtained output PISHG is equal to about 12% compared to the fundamental beam power. It is larger than for the silicon glasses treated at the same conditions and only a little less than in the azo-dye chromophore. The maximally-achieved second-order effective susceptibility is equal to about 1.89 pm V^{-1}. The optimal ratio between the fundamental and doubled frequency writing beam was equal to about 70, which corresponds to a writing power density of about 0.075 GW cm^{-2}.

In order to study the relaxation stability of the composites we have investigated the decay of the output PISHG with time. In figure 5 are presented the corresponding dependences versus the number of laser shots in the 125 Hz pulse repetition regime (sample **3**) after switching off the writing beam. One can see that for the optimal fundamental/writing beams ratio the output SHG does not decrease below 75% with respect to the initial grating. For higher values of the
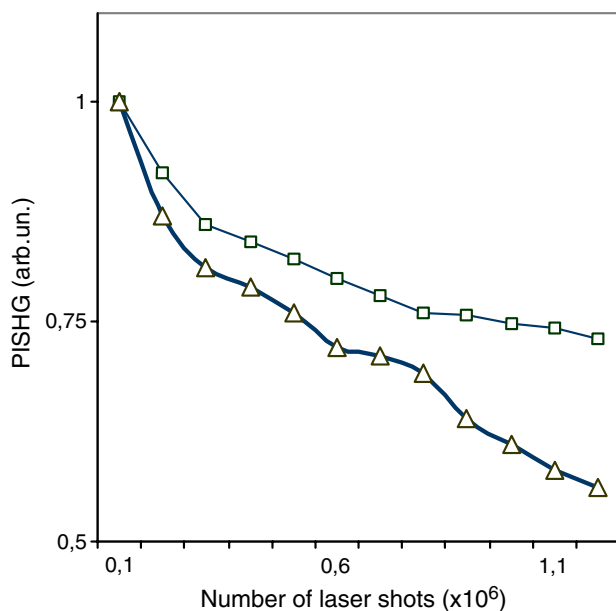
Figure 5. The time decay of the SHG for the writing beam for the chromophore **3** beam at different writing beam powers: □—writing beam power 0.074 GW cm^{-2}; △—writing beam power 0.10 GW cm^{-2}.
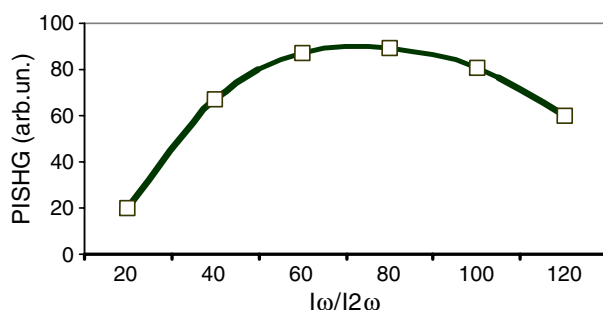
Figure 6. The dependence of the output photoinduced SHG versus the ratio of the fundamental to the doubled frequency writing beam for the composite containing chromophore **3**.

ratio this decay is substantially higher. So one can conclude that this ratio plays a substantial role in the observed SHG's stability of the composites.

For convenience, in figure 6 are presented the PISHG maxima dependences versus the fundamental/doubled frequency maxima (in particular, for sample **3** at the optimal concentration conditions). One can clearly see that the PISHG maximum is achieved for writing beam power density equal to about 0.075 GW cm^{-2}, which corresponds to the above-mentioned ratio of about 70.

Because the molecules are linearly elongated, one can expect that the directions of the particular dipole moments should be almost parallel. One can clearly see that there exists a clear peak in the position of the photoinduced SHG maximum for the writing 2ω beam. One can see also from figure 6 that the $\chi^{(2)}$-grating is different for the various peak powers $I_2(2\omega)$.

The efficiency of the photoinduced SHG increases with treatment time and reaches a certain steady-state value which is its maximum magnitude. However, there is a region of the values of $I_2(2\omega)$ for which the efficiency of the SHG initially increases with time, but then saturates and reaches the same steady-state value which is smaller than the maximum magnitude of the photoinduced SHG [21, 24].

Optically-polarized measurements have shown that in our experiment the induced electric field gratings have period ($L \approx 18$–26 μm) along the direction of the propagation of the radiation with doubled frequency but have the typical narrow size of the cross-section in the plane which is perpendicular to the direction of the propagation of beam (about 1.2 μm). The cross-section size of the induced field grating is formed by the convolution of the cross-section distributions of incident radiations with the fundamental and the doubled frequency. Therefore, it is somewhat less than the diameter of the incident beam of doubled frequency. The value of the absorption of the radiation with doubled frequency in an unperturbed OEA photocomposition is approximately $\alpha_2 \sim 10^{-3}$ cm^{-1}, so the matrix does not crucially disturb the observed dependences. From our experiment we have estimated the value of the electric field, which corresponds to the value of $\chi^{(2)}$, to be $\sim 10^2$–10^4 V cm^{-1}.

To gain an insight of the phenomenon we present below a short phenomenological description.

The spatial periodicity of a photoinduced field (3) with a period of q^{-1} creates the conditions for the occurrence of electrically induced SHG [25] on the attendant grating of the second-order susceptibility $\chi_{ijk}^{(2)} \sim \chi_{ijkl}^{(3)} E_{0l}$ and the process of the conversion of light in this grating is phase-matched.

The relaxation time of the writing field grating in the presence of the radiation with doubled frequency must be several orders less than in the presence of the radiation with fundamental frequency. In experiments we observed that the time of the erasure of the field grating by the light with fundamental frequency adds up to many hours and is near the dark time of the erasure of the field grating, while the time of the erasure by the light with doubled frequency adds up to some seconds.

One of possible mechanisms of the long-lived kinetics of the absorption of light in the region of the induced high electric field, in our opinion, can be the occurrence of the electrostrictive phonons and diffusion processes effectively depopulating the appropriate trapping levels [9, 14].

The mechanical stress second-rank tensor σ_{ij} induces a phonon displacement field with displacement vectors directed along the i and j directions. The considered phonons interact with the localized trapping states changing substantially their living times and polarizabilities. In particular there occur long-lived polaron (autolocalized phonon) states causing an anisotropy of the diffusion coefficient D. Its value depends on the type of composite.

As a consequence, the occupation of the trapping levels responsible for the electrostatically macropolarized states should decrease.

During illumination by the polarized light the diffusion coefficient D of the bound electron–phonon carriers decreases favouring additional polarization of the excited trapping levels [26]. The appearance of an additional number of trapping levels leads to the occurrence of a larger number of delocalized states within the forbidden energy gap. As a consequence it is possible to stabilize the decay of the SHG.

In our opinion one of the key factors favouring increasing second-order susceptibility is caused by the gradient of the electrostatic potentials of the polymer matrix and of the particular chromophore. One can guess that the subsequent search for materials with improved second-order properties should be directed towards materials possessing higher gradients of the local electrostatic electric field and corresponding dipole moments.

4. Conclusions

In conclusion, in the present paper it is experimentally demonstrated that optical poling in the stilbene-benzoate derivatives incorporated within the OEA photopolymer matrices give a long-lived optical $\chi^{(2)}$ grating of the composites at the ratio of the doubled frequency beam to the fundamental laser beam of about 1:70. The maximally achieved value of effective second-order susceptibility was equal to about 1.89 pm V^{-1}, which is substantially higher than in the inorganic glasses and only a little less than for the red azo-dye chromophores. However, compared with the former the long-lived stability is substantially higher, and in the optimal treatment regime (chromophore content about 6.5%) the corresponding optical grating parameters may be comparable with the better currently obtained samples. The quantum chemical calculations show a correlation of the obtained values of the optically-poled grating with the microscopic hyperpolarizabilities of the chromophore and the surrounding polymer matrices.

Molecules incorporated within the OEA matrices may be an efficient way for the creation of highly efficient non-linear optical materials. Due to the additional alignment of the photopolymer composite during the optical poling there exists the possibility of the creation of a long-lived stable grating, which would keep its properties even over several years.

References

 [1] Oesterberg U and Margulis W 1986 *Opt. Lett.* **12** 516
 [2] Stolen R H and Torn H W 1987 *Opt. Lett.* **12** 585
 [3] Matsuoka N, Kitaoka K, Si J, Fujita K and Hirao K 2000 *Opt. Commun.* **185** 467
 [4] Churikov V M and Hsu C-C 2001 *Opt. Commun.* **190** 367
 [5] Lopez-Lago E, Courders V, Griscom L, Smektala F and Barthelemy A 2001 *Opt. Mater.* **16** 413
 [6] Fischer M, Osman A E, Blanche P-A and Dumont M 2000 *Synth. Met.* **115** 139
 [7] Martin G, Toussaere E, Souilier L and Zyss J 2002 *Synth. Met.* **127** 49
 [8] Antonyuk B P 2000 *Opt. Commun.* **174** 427
 [9] Balakirev M K, Kityk I V, Smirnov V A and Vostrikova L I 2003 *Phys. Rev.* A **67** 023806
[10] Kyung J H and Lawandy N M 1994 *J. Opt. Soc. Am.* B **11** 355
[11] Si J, Kitaoka K, Qiu J, Mitsuyu T and Hirao K 1999 *Opt. Lett.* **24** 911
[12] Balakirev M K, Kityk I V, Smirnov V A and Vostrikova L I 2003 *Phys. Rev.* A **67** 023806
[13] Charra F, Kajzar F, Nunzi J-M, Raimond F and Idiart E 1993 *Opt. Lett.* **18** 419–25
[14] Sahraoui B, Kityk I V, Nguyen Phu X, Hudhomme P and Gorgues A 1999 *Phys. Rev.* B **59** 9229
[15] Kasperczyk J, Kityk I V, Kulesza M, Czerwinski M and Mervinskii R I 1998 *Mater. Chem. Phys.* **58** 7
[16] Ko C-W, Tao Y-T, Danel A, Krzeminska L and Tomasik P 2001 *Chem. Mater.* **6** 2441–6
[17] Siergrist A E 1967 *Helv. Chim. Acta* **50** 906
[18] Mervinskii R I, Kityk I V, Makowska-Janusik M, Matusiewicz M, Kasperczyk J and Straube J 1996 *Opt. Mater.* **6** 239
[19] Kityk I V, Kasperczyk J, Mervinskii R I and Jossi S 1996 *Mater. Lett.* **27** 233
[20] Sahraoui B, Kityk I V, Hudhomme P and Gorgues A 2001 *J. Phys. Chem.* B **105** 6295
[21] Baskin E M and Entin M V 1998 *JETP Lett.* **48** 601
[22] Sulimov V B 1992 *Sov. Phys.—JETP* **74** 932
[23] Balakirev M K, Vostrikova L I and Smirnov V A 2002 *Quantum Electron.* **32** 416–20
[24] Antonyuk B P and Antonyuk V B 2001 *Sov. J. Adv. Phys. Sci.* **171** 61–78
[25] Hickman J M, Gouveia E A, Gouveia-Neto A S and Dini D C 1994 *Opt. Lett.* **19** 1726
[26] Kityk I V 2003 *J. Phys. Chem.* B **107** 10087